Piotr GAS[1], Arkadiusz MIASKOWSKI[2], Dariusz DOBROWOLSKI[3]

AGH University of Science and Technology (1), University of Life Sciences in Lublin (2)
University College of Enterprise and Administration in Lublin (3)

doi:10.15199/48.2020.02.35

Modelling the tumor temperature distribution in anatomically correct female breast phantom

Abstract. *The presented paper focuses on a numerical analysis of temperature in the anatomical model of the female breast with a strictly defined level of power generated by the EMF source in pathological tissue saturated with ferrofluid. The aim of this study was to examine the effect of blood perfusion rate models on the resultant tumor temperature. The four tumor perfusion models were subjected to comparative analysis: constant, linear, nonlinear and completely free of blood flow. The authors have shown that taking into account the various temperature dependences of blood perfusion models within the treated tissue might play an important role in the complex process of female breast cancer treatment planning.*

Streszczenie. *Przedstawiona praca skupia się na numerycznej analizie temperatury w anatomicznym modelu gruczołu piersiowego kobiety o ściśle określonym poziomie mocy generowanej przez źródło PEM w patologicznej tkance nasyconej ferrofluidem. Celem tej pracy było zbadanie wpływu perfuzji krwi na wypadkową temperaturę guza. Analizie porównawczej poddano cztery modele perfuzji w guzie: stały, liniowy, nieliniowy oraz model całkowicie pozbawiony przepływu krwi. Autorzy pracy wykazali, że uwzględnienie różnych zależności temperaturowych dla modeli perfuzji krwi w leczonej tkance, może odgrywać istotną rolę w złożonym procesie planowania leczenia nowotworów piersi. (**Modelowanie rozkładu temperatury guza w naturalistycznym fantomie gruczołu piersiowego**)*

Keywords: hyperthermia, breast cancer, magnetic fluid, Pennes equation, temperature-dependent perfusion, power deposition, FEM.
Słowa kluczowe: hipertermia, rak piersi, ciecz magnetyczna, równanie Pennesa, modele perfuzji, osadzanie energii, MES.

Introduction

Nowadays, electromagnetic fields and electric currents of different frequencies and pulse shapes have found application in the treatment of various diseases [1, 2]. The usage of thermal effect in medical therapies [3, 4] has found proven efficacy in the treatment of cancer including breast cancer, which is the most frequently diagnosed carcinoma in women [5]. For this reason, new oncological treatments are being constantly sought that permanently kill tumor cells, reduce the patients' mortality rates and cancer recurrence, without resecting the entire breast tissue, which is extremely important from the point of view of the psychophysical condition of the female patients. One of the promising cancer therapies that is still in the phase of intensive clinical studies, is the so-called magnetic fluid hyperthermia (MFH) [6–8]. In this procedure, magnetic nanoparticles (MNPs), with specific physico-chemical properties, are delivered into the tumor site, and then they are heated to high therapeutic temperatures in the range of $41–46°C$ by RF-induced heating. The heat dissipated inside MNPs under the AC magnetic field activates irreversible biochemical changes in cancer cells, resulting in apoptosis or necrosis of malignant cells, while leaving intact healthy tissues surrounding the tumor. Importantly, sources of such fields can be various types of applicators, RF coils, microwave antennas [9–11]. However, the effectiveness of this method can be increased by combining it with targeted tumor therapy including both radio- and chemotherapy [12]. The different imaging or detection techniques for female breast tumors are also of great importance in oncomedicine [13, 14].

A potential clinical treatment planning can be assisted by computer modeling [15], where individual heating profiles of MNPs as well as the dose and concentration of magnetic material necessary to achieve a specific therapeutic effect in a given disease case can be determined by computer simulation [16]. The main limitation of magnetic hyperthermia treatment is meeting the following exposure criterion in the form $Hf < 4.85 \cdot 10^8$ A/m/s. This value is related to the pain threshold for induced eddy currents within the human trunk, however, weaker restrictions are allowed for smaller body parts subjected to radiation exposure. In the case of ferrofluid heating, a useful RF exposure range is often limited to the frequency of $f < 1$ MHz and to the magnetic field intensity of $H < 16$ kA/m [17]. Interestingly, MNPs are also employed in diversity of industrial applications [18].

To assess the effectiveness of MFH researchers often use both virtual and physical female breast phantoms [19–21]. The 3D heterogeneous, naturalistic, virtual female breast models seem to be the best solution for this purpose, however, due to the complex anatomical structure and long computation time, they are often replaced by simplified (semi-spherical or semi-ellipsoidal) models with a uniform internal structure [22–26, 35].

The presented paper neglects the important technical aspects of generating appropriate electromagnetic field (EMF), and focuses on the numerical analysis of temperature in the breast model, with a precisely defined level of power generated by the external EMF source in breast tumor tissue saturated with ferrofluid. The values of power dissipation in magnetic nanoparticles Q_{nano} are the result of the authors' experience [6] and previously performed calorimetric measurements of the ferrofluids based on magnetite aqueous solutions [7]. Of course, the value of this parameter obtained from *in vitro* studies must differ from *in vivo* measurements, where the actual tumor shape, perfusion as well as complicated interactions between magnetic nanoparticles (MNPs) and tumor tissue should be taken into account. Hence, the usage of the 3D anatomically corrected female breast model in current paper is fully justified.

The aim of this study was to examine the effect of blood perfusion rate models on the resultant temperature of breast tumor. What is important, the four tumor perfusion models were subjected to comparative analysis: constant (independent of temperature), linear, nonlinear and completely free of blood flow. The authors clearly showed that taking into account the different temperature dependences of blood perfusion rates within the treated tissue might play an important role in the complex treatment planning of female breast cancer.

Model Description and Basic Equations

In order to come to the real medical case as close as possible, the authors performed calculations on the 3D anatomical, heterogeneous phantom of the female breast created from the MR images by [19]. This model in different variants (degrees of complexity) was successfully used in our earlier works [6, 27]. The current virtual model of female breast consists of 227×299×162 voxels and assumes a heterogeneously dense of breast tissue at a level of 51–75%, which well reflecting the complex structure of breast gland.

a) b)

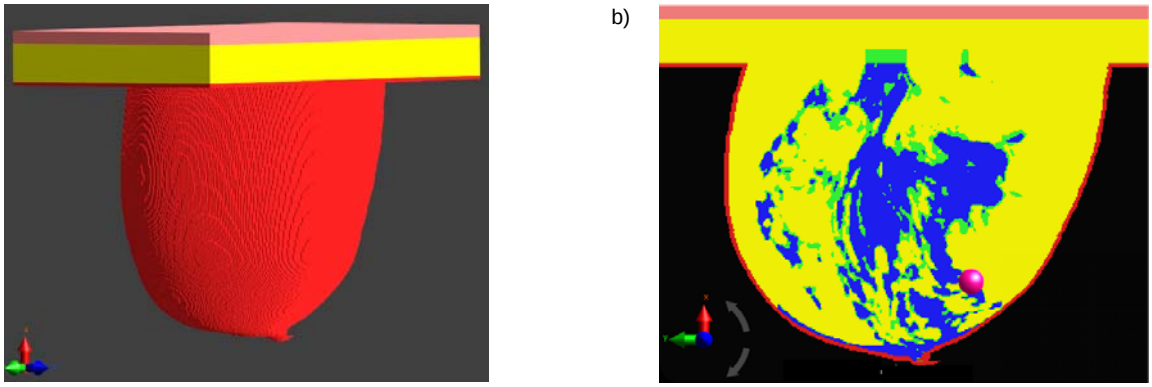

Fig. 1. a): The 3D female breast model, and b): its cross-section ($z = 0$) taking into account the tumor ($r = 10$ mm) and surrounding tissues

Therefore, it was possible to extract several basic tissues in the considered model, namely skin (red), muscles (orange), breast gland (blue), breast fat (yellow), fat (green), as well as tumor tissue (pink), as depicted in Fig. 1. Such a model. was analysed in the Cartesian coordinate system (x, y, z).

To determine the temperature distributions in modelled breast phantom, the modified bioheat transfer equation was employed, commonly known as the Pennes equation [28]:

$$\rho c \frac{\partial T}{\partial t} = \nabla \cdot (k \nabla T) + \rho Q_{\mathrm{m}} + Q_{\mathrm{nano}} + \rho_{\mathrm{b}} c_{\mathrm{b}} \rho \omega(T)(T_{\mathrm{b}} - T) \tag{1}$$

where ρ and ρ_{b} [kg/m^3] stand for the mass density, c and c_{b} [J/kg/K] – the specific heat, T and T_{b} [K] – the temperature of tissue and arterial blood, respectively. What is more, t [s] means the time, k [W/m/K] represents the tissue thermal conductivity, and $\omega(T)$ [mL/min/kg] means the temperature-dependent blood perfusion rate. Therefore, the perfusion source part $\rho_{\mathrm{b}} c_{\mathrm{b}} \rho \omega$ [W/m^3/K], also called heat-transfer rate (HTR), defines the power losses in unit temperature due to blood flow within individual tissues. In addition, Q_{m} [W/kg] is the heat generation rate due to tissue cells metabolism as well as Q_{nano} [W/m^3] specifies power losses due to magnetic nanoparticles according to the equation below [17]:

$$Q_{\mathrm{nano}} = \pi \mu_0 \chi'' H_0^2 f \tag{2}$$

where $\mu_0 = 4\pi \cdot 10^{-7}$ H/m stand for the permeability of free space, χ''(–) denotes the average out-of-phase component of AC susceptibility ($\underline{\chi} = \chi' - \mathrm{j}\chi''$) from MNPs. What is more, H_0 means the magnetic field intensity in given material, and f is the frequency of AC magnetic field.

The bio-heat equation (1) assumes the temperature dependence of blood flow through tumor, whose various models, namely strongly non-linear, linear, constant and without perfusion define the following equations [6, 29, 30]:

$$\omega(T) = \alpha + \beta \exp\left[-\frac{(T-37)^4}{\gamma} \right] \tag{3}$$

$$\omega(T) = \alpha_1 + \beta_1 T \tag{4}$$

$$\omega(T) = \alpha_0 \tag{5}$$

$$\omega(T) = 0 \tag{6}$$

where α, β, γ are constant coefficients, that exact numerical values are gathered in Table 1, and the corresponding $\omega(T)$ -distributions are shown in Fig. 2. It should be noticed, that all considered curves intersect at $T = 42$°C, i.e. for the temperature characteristic for magnetic hyperthermia treatment.

Table 1. Formulations for different tumor blood perfusion models

Model	Formula
non-linear	$\omega(T) = 0.4 + 0.4 \exp\left[-\frac{(T-37)^4}{880} \right]$
linear	$\omega(T) = -1.08 + 0.04T$
constant	$\omega(T) = 0.6$
no perfusion	$\omega(T) = 0$

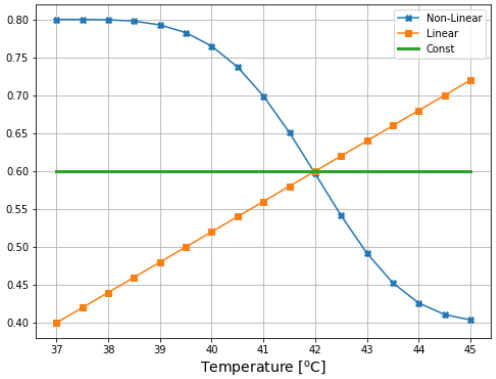

Fig. 2. Temperature-dependent characteristics of normalized tumor perfusion rates

The heat exchange between the breast skin surface and the external environment is determined by the Robin-type boundary condition, namely [10]:

$$\mathbf{n} \cdot (-k_{\mathrm{skin}} \nabla T) = h(T_{\mathrm{ext}} - T) \tag{7}$$

where k_{skin} [W/m/K] indicates the thermal conductivity of the skin, and h [W/(m^{2}K)] is the so-called heat transfer coefficient that is associated with the breast skin layer. In addition, T_{ext} means the temperature of the breast surrounding, and $\mathbf{n}$ is the normal vector to the breast surface.

Simulation Results

Based on the previous author's the experiences [6] and performed calorimetric measurements [7], it was assumed that the power density generated in magnetic nanoparticles (placed in the tumor) under external AC magnetic field was set at the level of $Q_{\mathrm{nano}} = 109$ kW/m^3. The excitation was turned off after the exposure time $t = 30$ min. The external temperature was established at $T_{\mathrm{ext}} = 25$°C, and the heat transfer coefficient was chosen to be $h = 9.5$ W/(m^2·K). Importantly, the initial temperature of the breast tissues was $T_0 = 37$°C and the arterial blood temperature T_{b} is assumed at the same level as the female breast core temperature T_0.

Thermal parameters of different breast tissues used in the simulation were taken from the Information Technologies in Society (IT'IS) database [31] and summarized in Table 2. It should be noted that the physical parameters of the tumor correspond to the parameters of muscle tissue, except for the very high compared to other tissues value of metabolic heat generation $Q_m = 100$ W/kg characteristic for malignant cells as well as temperature-dependent perfusion rate $\omega(T)$ defined in Table 1. What is important, the outlined thermal problem was numerically solved using the finite element method (FEM) with commercially available tool of Sim4Life software [32].

Table 2. Tissue parameters employed in the Pennes equation [31]

Quantity	Blood	Breast fat	Breast gland
Q_m [W/kg]	0	0.728	2.323
ρ_b, ρ[kg/m^3]	1050	911	1041
c_b, c [J/kg/K]	3617	2348	2960
k [W/m/K]	0.5169	0.209	0.334
ω [mL/min/kg]	10 000	47	150
HTR [W/m^3/K]	$6.646 \cdot 10^5$	2710	9974

Quantity	Fat	Muscle	Skin	Tumor
Q_m [W/kg]	0.506	0.906	1.648	100
ρ[kg/m^3]	911	1090	1109	1090
c [J/kg/K]	2348	3421	3391	3421
k [W/m/K]	0.211	0.495	0.372	0.495
ω [mL/min/kg]	32.71	36.74	106	Table 1
HTR [W/m^3/K]	1886	2536	7468	$\rho_b c_b \rho \omega$

Fig. 3 illustrates a sample xy-cross section temperature distributions for different tumor perfusion models, including constant, linear, nonlinear, and non-perfusion models after 30-min-period of exposure, when the exciting AC magnetic field is vanished (Q_{nano} has a zero value). As expected, the highest temperatures were recorded in the tumor site.

The transient profiles of temperature in tumor centre for all analysed models are curved in Fig. 4. The fastest the tumor temperature reached the steady-state in the case of the tumor model with linear perfusion, and the most slowly non-perfused tumor was heated up. Interestingly, the similar levels of temperature, namely 44.8°C, 44.1°C and 44.5°C, have been observed for constant, linear and non-linear perfusion models, respectively. Moreover, the tumor heat accumulation, at level of almost 49°C, was reported for the non-perfusion model, which is due to the damage of tumor cooling mechanisms by circulating blood. Such a situation occurs especially within the dense-vascularized solid tumors, which dysfunctional blood vessels have completely lost their thermoregulatory properties [33, 34].

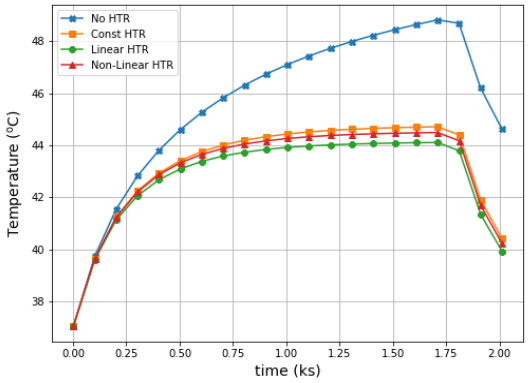

Fig. 4. The comparison of time dependences inside centre of tumor for different tumor perfusion models, namely: constant (orange), linear (green), non-linear (red), and without blood perfusion (blue)

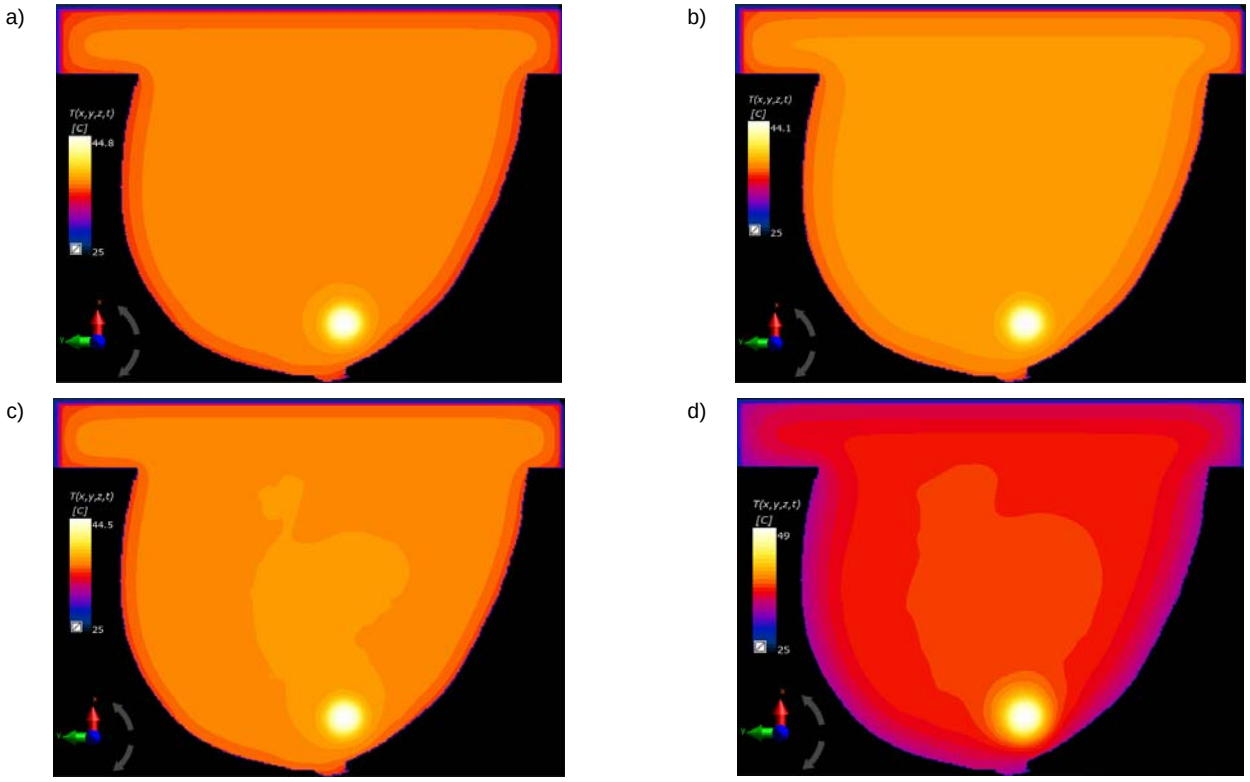

Fig. 3. Temperature distributions in the modelled female breast phantom after treatment time equal to $t = 30$ min for various tumor perfusion models: a) constant, b) linear, c) non-linear, and d) without blood perfusion

Summary

The work focuses on numerical analysis of the modified Pennes equation to assess the temperature profiles of a female breast tumor with temperature-dependent blood perfusion. In order to get as close to the real medical case as possible, the simulations were carried out on a realistic female breast phantom using the finite element method. For simplicity, a defined level of power deposition in magnetic nanoparticles (MNPs) was assumed at $109\ \mathrm{kW/m^3}$, based on the previous experience of the authors in magnetic fluid hyperthermia calorimetric measurements. The four tumor perfusion models were subjected to comparative analysis: constant (independent of temperature), linear, nonlinear and completely free of blood flow. As expected, the highest temperatures were recorded in the tumor site. The fastest the tumor temperature reached the steady-state in the case of the tumor with linear perfusion, and the most slowly for non-perfused tumor. Simultaneously, in the model without blood flow the temperature achieved the most significant level. Thus, the authors have showed that selection of proper blood perfusion model might play an important role in the complex treatment procedure of female breast cancer.

***Authors**: dr inż. Piotr Gas, PhD, AGH University of Science and Technology, Department of Electrical and Power Engineering, al. Mickiewicza 30, 30-059 Krakow, E-mail: piotr.gas@agh.edu.pl, dr hab. inż. Arkadiusz Miaskowski (corresponding author), PhD, University of Life Sciences in Lublin, Department of Applied Mathematics and Computer Sciences, ul. Akademicka 13, 20-950 Lublin, Poland, E-mail: arek.miaskowski@up.lublin.pl, dr Dariusz Dobrowolski, University College of Enterprise and Administration in Lublin, Faculty of Technical Sciences, ul. Bursaki 12, 20-150 Lublin Poland, E-mail: d.dobrowolski@wspa.pl*

REFERENCES

[1] Wyszynska E., et al., Electrotherapy – Therapy Possibilities Across the Ages and Today, *2019 Applications of Electromagnetics in Modern Engineering and Medicine (PTZE)*, IEEE, (2019), 263-266. DOI: 10.23919/PTZE.2019.8781703

[2] Syrek P., Uncertainty Problem as Illustrated by Magnetotherapy, *Applied Computational Electromagnetics Society Journal*, 34 (2019), No. 9, 1445-1452.

[3] Woesner M.E., What is old is new again: The use of whole-body hyperthermia for depression recalls the medicinal uses of hyperthermia, fever therapy, and hydrotherapy, *Current Neurobiology*, 10 (2019), No. 2, 56-66.

[4] Gas P., Wyszkowska J., Influence of multi-tine electrode configuration in realistic hepatic RF ablative heating, *Archives of Electrical Engineering*, 68 (2019), No. 3, 521-533.

[5] Plawiak-Mowna A., et al., Occupational EMF exposure and risk of breast cancer, *Przeglad Elektrotechniczny*, 93 (2017), No. 1, 177-180.

[6] Sawicki B., and Miaskowski A., Nonlinear higher-order transient solver for magnetic fluid hyperthermia, *Journal of Computational and Applied Mathematics*, 270 (2014), 143-151.

[7] Gas P., and Miaskowski A., Specifying the ferrofluid parameters important from the viewpoint of Magnetic Fluid Hyperthermia, in *2015 Selected Problems of Electrical Engineering and Electronics (WZEE)*, IEEE, (2015), 1-6. DOI: 10.1109/WZEE.2015.7394040

[8] Lanier O.L., et al., Evaluation of magnetic nanoparticles for magnetic fluid hyperthermia, *International Journal of Hyperthermia*, 36 (2019), No. 1, 687-701.

[9] Michalowska J., Wac-Wlodarczyk A., The analysis of an absorption rate in view of electromagnetic exposure effects exemplified by the breast cancer, *European Journal of Medical Technologies*, 2 (2017), No. 15, 29-36.

[10] Gas P., Miaskowski A., SAR optimization for multi-dipole antenna array with regard to local hyperthermia, *Przeglad Elektrotechniczny*, 95 (2019), No. 1, 17-20.

[11] Kumari et al., SAR analysis of directive antenna on anatomically real breast phantoms for microwave holography, *Microwave and Optical Technology Letters* (2019). DOI: 10.1002/mop.32037

[12] Singh S.P. Microwave Thermotherapy and its Clinical Applications, in *2019 URSI Asia-Pacific Radio Science Conference (AP-RASC)*, IEEE, (2019), 1-4.

[13] Ramu S., et al., Diagnosis of Cancer Using Hybrid Clustering and Convolution Neural Network from Breast Thermal Image, *Journal of Testing and Evaluation*, 47 (2019), No. 6, 3975-3987.

[14] El Fatimi A., et al., UWB antenna with circular patch for earley breast cancer detection, *Telkomnika*, 17 (2019), No. 5, 2370-2377.

[15] Prasad B., et al., Role of Simulations in the Treatment Planning of Radiofrequency Hyperthermia Therapy in Clinics, *Journal of Oncology*, 2019 (2019), 9685476.

[16] Bekovic M., et al., Numerical Model for Determining the Magnetic Loss of Magnetic Fluids, *Materials*, 12 (2019), No. 4, 591.

[17] Kurgan E., and Gas P., Simulation of the electromagnetic field and temperature distribution in human tissue in RF hyperthermia, *Przeglad Elektrotechniczny*, 91 (2015), No. 1, 169-172. DOI: 10.15199/48.2015.01.37

[18] Szczech M., Influence of Selected Parameters on the Reseal Instability Mechanism in Magnetic Fluid Seals, *Journal of Magnetics*, 24 (2019), No. 1, 32-38.

[19] Gill H.S., et al., Computational study on effect of microwave induced hyperthermia on breast tumor, *International Journal of Mechanical and Production Engineering Research and Development*, 7 (2017), No. 5, 343-358.

[20] Burfeindt M.J., et al., MRI-derived 3-D-printed breast phantom for microwave breast imaging validation, *IEEE Antennas and Wireless Propagation Letters*, 11 (2012), 1610-1613.

[21] Joachimowicz N., et al., Anthropomorphic breast and head phantoms for microwave imaging, *Diagnostics*, 8 (2018), No. 4, 85.

[22] Patil H.M., Maniyeri R., Finite difference method based analysis of bio-heat transfer in human breast cyst, *Thermal Science and Engineering Progress*, 10 (2019), 42-47.

[23] Balusu, et al., Modelling bio-heat transfer in breast cysts using finite element analysis. In: *2014 International Conference on Informatics, Electronics & Vision (ICIEV)*, IEEE, (2014), 1-4.

[24] Gambin B., et al.,Ultrasonic Measurement of Temperature Rise in Breast Cyst and in Neighbouring Tissues as a Method of Tissue Differentiation, *Archives of Acoustics*, 41 (2016), No. 4, 791-798.

[25] Sobkiewicz P., et al., Estimating the temperature of breast malignant tissue during microwave ablation process, *Przeglad Elektrotechniczny*, 95 (2019), No. 12, 212-215.

[26] Singh S., Repaka R., Effect of different breast density compositions on thermal damage of breast tumor during radiofrequency ablation, *Applied Thermal Engineering*, 125 (2017), 443-451.

[27] Michalowska-Samonek J., Miaskowski A., Wac-Wlodarczyk A., Numerical models of human breast, *Przeglad Elektrotechniczny*, 85 (2009), No. 12, 125-127.

[28] Pennes H.H, Analysis of Tissue and Arterial Blood Temperatures in the Resting Human Forearm, *Journal of Applied Physiology*, 85 (1998), No. 1, 5-34.

[29] Lang M, et al., Impact of nonlinear heat transfer on temperature control in regional hyperthermia, *IEEE Transactions on Biomedical Engineering*, 46 (1999), 1129-1138.

[30] Kengne E., Lakhssassi A., Analytico-numerical study of bio-heat transfer problems with temperature-dependent perfusion, *The European Physical Journal Plus*, 130 (2015), No. 5, 89.

[31] Hasgall P.A., et al., IT'IS Database for thermal and electromagnetic parameters of biological tissues, Version 4.0, May 15th 2018.

[32] https://www.zurichmedtech.com/sim4life/ [12.10.2018]

[33] Kashkooli, et al., Image-based spatio-temporal model of drug delivery in a heterogeneous vasculature of a solid tumor-Computational approach, *Microvascular Research*, 123 (2019), 111-124.

[34] Muntoni G., et al., A Blood Perfusion Model of a RMS Tumor in a Local Hyperthermia Multi-Physic Scenario: A Preliminary Study, *IEEE Journal of Electromagnetics, RF and Microwaves in Medicine and Biology*, 3 (2019), No. 1, 71-78.

[35] Paruch M., Mathematical Modeling of Breast Tumor Destruction using Fast Heating during Radiofrequency Ablation, *Materials*, 13 (2020), No. 1, 136.